

Published in final edited form as:

*Circ Heart Fail.* 2012 January ; 5(1): 116–125. doi:10.1161/CIRCHEARTFAILURE.111.964783.

## Akt1–Mediated Skeletal Muscle Growth Attenuates Cardiac Dysfunction and Remodeling After Experimental Myocardial Infarction

Satoshi Araki, MD, Yasuhiro Izumiya, MD, PhD, Shinsuke Hanatani, MD, Taku Rokutanda, MD, Hiroki Usuku, MD, PhD, Yuichi Akasaki, MD, PhD, Toru Takeo, PhD, Naomi Nakagata, PhD, Kenneth Walsh, PhD, and Hisao Ogawa, MD, PhD

Department of Cardiovascular Medicine (S.A., Y.I., S.H., T.R., H.U., H.O.), Faculty of Life Sciences, Kumamoto University, Kumamoto, Japan; Molecular Cardiology (Y.A., K.W.), Whitaker Cardiovascular Institute, Boston University School of Medicine, Boston, MA; Division of Reproductive Engineering (T.T., N.N.), Center for Animal Resources and Development, Kumamoto University, Kumamoto, Japan

### Abstract

**Background**—It is appreciated that aerobic endurance exercise can attenuate unfavorable myocardial remodeling following myocardial infarction. In contrast, little is known about the effects of increasing skeletal muscle mass, typically achieved through resistance training, on this process. Here, we utilized transgenic (TG) mice that can induce the growth of functional skeletal muscle by switching Akt1 signaling in muscle fibers to assess the impact of glycolytic muscle growth on post-myocardial infarction cardiac remodeling.

**Methods and Results**—Male-noninduced TG mice and their nontransgenic littermates (control) were subjected to left anterior coronary artery ligation. Two days after surgery, mice were provided doxycycline in their drinking water to activate Akt1 transgene expression in a skeletal muscle-specific manner. Myogenic Akt1 activation led to diminished left ventricular dilation and reduced contractile dysfunction compared with control mice. Improved cardiac function in Akt1 TG mice was coupled to diminished myocyte hypertrophy, decreased interstitial fibrosis, and increased capillary density. ELISA and protein array analyses demonstrated that serum levels of proangiogenic growth factors were upregulated in Akt1 TG mice compared with control mice. Cardiac eNOS was activated in Akt1 TG mice after myocardial infarction. The protective effect of skeletal muscle Akt activation on cardiac remodeling and systolic function was abolished by treatment with the eNOS inhibitor L-NAME.

**Conclusions**—Akt1–mediated skeletal muscle growth attenuates cardiac remodeling after myocardial infarction and is associated with an increased capillary density in the heart. This improvement appears to be mediated by skeletal muscle to cardiac communication, leading to activation of eNOS-signaling in the heart.

### Keywords

angiogenesis; exercise training; myocardial infarction; nitric oxide synthase; remodeling heart failure

Copyright © 2012 American Heart Association. All rights reserved© 2011 American Heart Association, Inc.

Correspondence to Yasuhiro Izumiya, MD, PhD, Department of Cardiovascular Medicine, Faculty of Life Sciences, Kumamoto University, 1-1-1 Honjo, Kumamoto, Kumamoto 860-8556, Japan. izumiya@kumamoto-u.ac.jp.

The online-only Data Supplement is available with this article at <http://circheartfailure.ahajournals.org/lookup/suppl/doi:10.1161/CIRCHEARTFAILURE.111.964783/-/DC1>.

Loss of skeletal muscle mass is frequently observed in patients with endstage chronic heart failure (CHF). It is well-recognized that skeletal muscle wasting is a strong independent risk factor for mortality in these patient populations.<sup>1</sup> A good correlation between lean muscle mass and exercise capacity has been found in patients with CHF.<sup>2</sup> Therefore, maintaining or increasing skeletal muscle mass could be beneficial in patients with CHF.

Conventional endurance training leads to an increase in the proportion of slow/oxidative fibers, which are high in mitochondrial content.<sup>3</sup> This type of exercise training elicits a variety of metabolic and morphological responses in skeletal muscle, including mitochondrial biogenesis.<sup>4</sup> Multiple lines of clinical evidence indicate that decreased percentage of oxidative fibers, mitochondrial dysfunction, and vascular rarefaction are prominent features of skeletal muscle in patients with CHF.<sup>5</sup> It is widely held that aerobic exercise training improves functional capacity and prognosis in patients with CHF.<sup>6</sup> Therefore, endurance training intended to increase oxidative fiber function is recognized as rational treatment strategy for CHF patients.<sup>7</sup>

Although high intensity treadmill exercise can have a modest effect in promoting muscle growth,<sup>8</sup> lean muscle mass is typically developed through resistance exercise training. Resistance exercise training is predominantly associated with an increase in protein synthesis and hypertrophy of fast/glycolytic fibers.<sup>9</sup> This type of exercise promotes gains in maximal force output but has minimal effects on muscle fiber phenotype transformation.<sup>10</sup> Recent work has shown that increased skeletal muscle mass and glycolytic capacity can improve body composition and systemic metabolic parameters.<sup>11,12</sup> Resistance training may also promote favorable effects on cardiac function and exercise capacity, and this type of training is now recommended as a complementary exercise modality for patient with cardiovascular disease.<sup>13</sup> Whereas it is widely appreciated that heart failure leads to muscle wasting,<sup>14</sup> a condition referred to as “cardiac cachexia,” it is unknown whether the reverse is true; can an increase in lean muscle mass improve cardiac function in the setting of heart failure?

The Akt family of serine-threonine protein kinases are functionally redundant signaling molecules that are activated by various extracellular stimuli through the phosphatidylinositol 3-kinase pathway. Numerous studies have implicated Akt signaling in the control of organ size and cellular hypertrophy.<sup>15</sup> The Akt signaling pathway is preferentially activated in skeletal muscle in response to anabolic stimuli and resistance training,<sup>9,16,17</sup> suggesting that Akt signaling may function as an important modulator of lean muscle mass through its ability to promote skeletal muscle hypertrophy and inhibit atrophy.<sup>18</sup> Consistent with these experimental observations, cardiac cachexia is associated with reduced Akt signaling in skeletal muscle tissue.<sup>19</sup>

In the present study, we utilized a conditional transgenic (TG) mouse model that can reversibly grow functional skeletal muscle by switching Akt1 signaling specifically in skeletal muscle following permanent left anterior descending coronary artery (LAD) ligation to elucidate the role of fast/glycolytic skeletal muscle growth in the control of cardiac remodeling after the mouse model of myocardial infarction (MI). We have previously reported that this model of Akt1 overexpression in skeletal muscle leads to the selective growth of glycolytic, type IIb skeletal muscle hypertrophy.<sup>20</sup> This muscle is functional in that mice display an increase in grip strength, but spontaneous ambulatory activity and running performance of Akt1 TG mice is lower than that of control mice.<sup>20</sup> Consistent with this phenotype, we have shown that transcripts for muscle-enriched glycolytic genes are significantly upregulated, whereas oxidative genes are reduced in Akt1 TG mice.<sup>20</sup> Here, we demonstrate that Akt1-mediated, glycolytic skeletal muscle growth increases capillary

growth in the myocardium and attenuates cardiac remodeling after MI. Skeletal muscle growth also increased in the cardiac eNOS signaling pathway, and inhibition of eNOS abolished the protective effects of muscle growth on post-MI cardiac remodeling.

## Methods

### Skeletal Muscle-Specific Conditional Akt1 TG Mice

The M-creatine kinase (MCK)-rtTA TG mice<sup>21</sup> were crossed with TRE-myrAkt1 TG mice<sup>22</sup> to generate double TG mice (Akt1 TG mice).<sup>20</sup> Mice were maintained on mixed genetic backgrounds of C57BL/6J for MCK-rtTA TG and FVB and C57BL/6 for TRE-myrAkt1 TG mice and were bred to produce each set of Akt1 TG experimental mice. The MCK promoter construct used in the driver line is mutated, and transgene expression is expressed in a subset of muscle, but no expression occurs in heart.<sup>19,21</sup> For Akt1 transgene expression, Akt1 TG mice were treated with doxycycline (DOX) in drinking water, and DOX water was removed to repress the transgene expression. MCK-rtTA single TG littermates were used as controls and treated with DOX in the same manner as Akt1 TG mice. Measurements of body composition were made by quantitative magnetic resonance, as described previously.<sup>23</sup> In some experiments, mice were given 1 mg/mL L-NAME (Dojindo) in drinking water at 2 days after MI or sham operation. Blood pressure of conscious mice was measured by tail-cuff method (MK-2000ST, Muromachi, Japan) every 2 weeks. Serum nitrogen oxide was measured by Nitrate/Nitrite Colorimetric Assay Kit (Cayman Chemical Company).

### Mouse Model of Myocardial Infarction

Control and Akt1 TG mice at the ages of 10 to 12 weeks were anesthetized with sodium pentobarbital (50 mg/kg intraperitoneally). The adequacy of anesthesia was monitored by the stability of blood pressure and heart rate by tail-cuff method and the stability of respiration. The trachea was cannulated with a polyethylene tube connected to a respirator with a tidal volume of 0.6 mL (110/min). A left thoracotomy was performed between the 4th and 5th ribs. The pericardial tissue was removed, and LAD was visualized under a microscope and permanently ligated with 8-0 silk sutures.<sup>24</sup> Sham-treated mice underwent surgery but not LAD ligation. DOX treatment started at 2 days after surgery. Survival of mice after MI was evaluated using the Kaplan-Meier method. Survived mice were euthanized after 2 or 4 weeks following DOX treatment. Mice were anesthetized with overdose pentobarbital, and hearts and skeletal muscle were rapidly excised and freeze-clamped for subsequent analyses. All procedures were performed in accordance with the Kumamoto University animal care guidelines (approval reference No. B23-206), which conformed to the Guide for the Care and Use of Laboratory Animals, published by the US National Institutes of Health (NIH Publication No. 85-23, revised 1996).

### Echocardiography

A transthoracic ultrasound cardiogram was performed using a Xario system (Toshiba, Tokyo, Japan), equipped with a 12-MHz linear array transducer. M-mode images were recorded from the short-axis view at the high papillary muscle level. Left ventricular end-diastolic dimension (LVED), end-systolic dimension, intraventricular septum, and posterior wall thickness were measured. Fractional shortening (% FS) was calculated using the following equation: % FS=(LVED-end-systolic dimension)/LVED×100. All recordings were performed in conscious mice. All echocardiography was performed by investigators who were blinded to the identity of the mouse genotype.

### Hemodynamic Measurements

Left ventricular contractile performance was determined 4 weeks after DOX treatment, as described previously.<sup>25</sup> In brief, a 1.4F catheter tip micromanometer (Millar Instruments) was percutaneously introduced into the carotid artery and gently advanced into the left ventricular cavity in mice under pentobarbital anesthesia (25 mg/kg single intraperitoneally injection). Pressure waves were recorded and analyzed with LabChart 7 Pro software (AD Instruments).

### Quantitative Real-Time PCR

Total RNA was prepared with a Qiagen RNeasy fibrous minikit, using the protocol supplied by the manufacturer, and cDNA was produced using ThermoScript RT-PCR Systems (Invitrogen, Carlsbad, CA). Quantitative real-time PCR was performed, as described previously.<sup>25</sup> Transcript expression levels were determined as the number of transcripts relative to those for 36B4 and normalized to the mean value from control hearts. Table 1 lists the primer sequences used in this study.

### Western Blot Analysis

Western blotting was performed with an SDS-PAGE Electrophoresis System, as described previously.<sup>25</sup> Primary antibody used were: phospho-eNOS (Ser 1177, p-eNOS), total-eNOS (t-eNOS), and GAPDH from Cell Signaling Technology; VEGF-A from Abcam;  $\alpha$ -tubulin from Calbiochem.

### Histological Analysis

Mice were euthanized and heart tissue was obtained at 2 weeks after MI. Myocardial tissues were fixed in 4% paraformaldehyde, dehydrated and embedded in paraffin. To determine the infarct size, sections were stained with Masson's trichrome. Total LV circumference was calculated as the sum of endocardial and epicardial segment lengths from all sections. Infarct size was calculated as total infarct circumference divided by total LV circumference. Capillary density was assessed by CD31 staining of tissue sections in the peri-infarct zone, as described previously.<sup>24</sup> Myocardial fibrosis and capillary density was quantified using Lumina Vision version 2.2 analysis software.

### Angiogenesis Antibody Array Analysis

The expression profile of 53 angiogenesis-related proteins was analyzed with mouse angiogenesis antibody arrays (R&D Systems Inc, Minneapolis, MN). Blocking, hybridization of the array filters, washing conditions, and chemiluminescent detection steps were performed according to the instructions supplied by the manufacturer.

### Statistical Analysis

All data are presented as mean $\pm$ SEM. The differences among groups were evaluated by using linear mixed effects models with measurements values as response variable, control/TG, and sham/MI, and these interactions as fixed effect and the parents as random effects. In multiple comparison tests, probability values were adjusted by Bonferroni method. Animal survival was evaluated by the Kaplan-Meier method, and the log-rank test was used to compare survival curves between MI-operated WT and MI-operated TG groups. Western blot densities were analyzed with Student *t* test. The significance level of a statistical hypothesis test was 0.05.

## Results

### Akt1–Mediated Skeletal Muscle Growth Attenuates Cardiac Dysfunction After MI

To investigate the relationships between skeletal muscle growth and cardiac remodeling, control (nontransgenic) and noninduced Akt1 TG mice were subjected to sham surgery or permanent LAD ligation to induce MI (Figure 1A). At 2 days following surgery and immediately before muscle-specific transgene induction with DOX, both control and Akt1 TG mice exhibited a progressive increase in LVED and a decrease in % FS relative to sham operated mice (Figure 1B). At the time of these baseline measurements, mice were provided with DOX in their drinking water. Mice were then harvested at either 2 or 4 weeks after DOX treatment to assess the progress of heart failure.

In this inducible transgenic system, Akt1 transgene was detected in skeletal muscle but not in the heart, in response to DOX treatment (Figure 1C). Transgene-induced skeletal muscle growth, as assessed by analysis of the gastrocnemius muscle weight/body weight (BW) ratio, was increased at both 2 and 4 weeks after DOX treatment, and LAD ligation did not affect this parameter (Figure 1D). Whereas gastrocnemius muscle growth was substantial, the mutated MCK promoter used in these studies is expressed in a subset of myofibers (such as gastrocnemius, tibialis anterior, and quadriceps muscle), and no transgene expression nor growth of other muscle groups including soleus and extensor digitorum extensor is observed.<sup>21</sup> Thus, the overall extent of muscle growth in this model is modest, with an increase in lean mass of approximately 5% as assessed by QMR (Figure 1E).

No significant difference occurred in the survival frequencies after MI between control and Akt1 TG mice (Figure 1F). Mortality in this model mostly occurred within 10 days of surgery, which was mainly caused by cardiac rupture. Death from heart failure was rare in our experimental model, and only 1 additional death was observed until the termination of the experiment at 4 weeks after DOX treatment. BW and heart rate did not differ between control and Akt1 TG mice at 4 weeks after DOX treatment in MI or sham treatment groups (Table 2).

Echocardiographic examination revealed that induction of the Akt1 transgene for 2 or 4 weeks in skeletal muscle led to a decrease in LVED and end-systolic dimension (Figure 2A). The protective effect of skeletal muscle Akt1 expression on cardiac function and remodeling was more apparent at 4 weeks than at 2 weeks after transgene activation, resulting in a statistically significant increase in % FS at the latter time point. DOX treatment of control mice had no effect on LV dimension and function in sham-operated mice at these time points.

Systolic arterial pressure was significantly decreased in both control and Akt1 TG mice at 4 weeks after DOX treatment compared with sham-treated mice, but there was no statistical difference between the control and Akt1 TG mice (Figure 2B); however, left ventricular systolic function, reflected by  $dp/dt_{max}$ , was improved in Akt1 TG mice at 4 weeks after DOX treatment (Figure 2B).

### Akt1–Mediated Skeletal Muscle Growth Prevents Cardiac Hypertrophy in Response to MI

Cardiac tissue sections were stained with Masson's trichrome to calculate infarct size in control and DOX-treated, skeletal muscle-specific Akt1 TG mice. The ratio of total infarct size to total LV circumference was the same in control and Akt1 TG mice. As shown in Figure 3A, the increase in heart weight/BW ratio at 2 weeks after DOX treatment was significantly smaller in Akt1 TG mice than that in control ( $5.0 \pm 0.1$  versus  $5.5 \pm 0.1$  mg/g,  $P=0.0332$ ), and the difference became more apparent at 4 weeks after DOX treatment ( $4.8 \pm 0.4$  versus  $5.8 \pm 0.2$  mg/g,  $P=0.0088$ ). No significant difference in heart weight/BW

ratio was observed in sham-operated control versus Akt1 TG mice. Analysis of the cardiomyocyte cross-sectional area in myocardial sections of remote areas to the infarct revealed that cardiomyocyte hypertrophy in response to MI was smaller in Akt1 TG mice than in control mice (Figure 3B). MI led to an increase in the expression of the fetal-type cardiac gene BNP, and this upregulation was also attenuated in Akt1 TG mice compared with control at 2 weeks after DOX treatment (Figure 3C). Akt1 activation in skeletal muscle did not detectably affect BNP expression in the hearts of sham-operated mice. Lung wet weight/BW ratio at 2 and 4 weeks after DOX treatment was significantly decreased in Akt1 TG mice compared with that in control mice, indicating diminished pulmonary congestion in mice expressing the skeletal muscle transgene (Figure 3D).

### **Akt1 TG Mice Displayed Decreased Interstitial Fibrosis and Increased Myocardial Capillary Density After MI**

Myocardial interstitial fibrosis in the border and remote zone was assessed in Masson S trichrome-stained tissue sections (Figure 4A). Interstitial fibrosis was significantly decreased in Akt1 TG mice compared with control mice after MI. Little or no fibrosis could be detected in either Akt1 TG or control mice that underwent sham surgeries. Consistent with these observations, collagen I and III gene expression in the border zone was significantly decreased in the hearts of Akt1 TG mice compared with control mice (Figure 4A). Akt1 activation in skeletal muscle did not detectably affect collagen I and III expression in the hearts of sham-operated mice.

Capillary density was assessed in histological sections corresponding to the infarct border and remote zones (Figure 4C). CD31-positive cells in the heart increased following LAD ligation, and this increase was enhanced by Akt1 transgene activation in skeletal muscle. Capillary density was unaffected by Akt transgene induction in sham-operated mice.

### **Akt1-Mediated Skeletal Muscle Growth Increases Angiogenesis Growth Factor Levels in Serum**

Because it is reported that myogenic Akt signaling controls angiogenic growth factor synthesis,<sup>26</sup> we examined the circulating angiogenic factors by the mouse angiogenesis protein array and found that serum VEGF-A, FGF-1, FGF-2, and SDF-1 levels were significantly upregulated in Akt1 TG mice compared with control mice at 2 weeks after DOX treatment (Figure 5A). Among them, the increase in serum VEGF-A concentration was validated by ELISA ( $87 \pm 7$  versus  $69 \pm 11$  pg/mL,  $n=6$ ,  $P=0.0229$ ). VEGF-A protein expression was significantly increased in skeletal muscle of Akt1 TG mice than that in control mice after 2 or 4 weeks DOX treatment (Figure 5B). There was no change in the cardiac expression of VEGF between control and Akt1 TG hearts (data not shown).

### **Therapeutic Effects of Akt1-Mediated Muscle Growth on Cardiac Remodeling Is Blocked by the Treatment With NOS Inhibitor**

Next, we assessed whether Akt1-mediated skeletal muscle growth and subsequent angiogenic factors' upregulation could affect intracellular signaling in the heart after MI. As shown in Figure 6A, the activating phosphorylation of eNOS at Ser1177, a downstream effector of angiogenic growth factor signaling,<sup>27</sup> was significantly increased in the border zone and remote zone of the myocardium at 2 weeks after DOX treatment. Cardiac eNOS activation in Akt1 TG mice was sustained in the remote zone of myocardium at 4 weeks after DOX treatment.

To examine whether the activation of eNOS is causally linked to improved cardiac remodeling, control and Akt1 TG mice were treated with L-NAME, a NOS inhibitor, for 4 weeks (Figure 6B). Chronic L-NAME treatment significantly decreased serum NOx



concentration in control and Akt1 TG mice (online-only Supplemental Figure 1A). Systolic blood pressure was significantly increased in both sham- or MI-treated mice at 2 or 4 weeks after L-NAME treatment compared with day 0, but there was no statistical difference in this parameter between the control and Akt1 TG mice (online-only Supplemental Figure 1B). Akt1-mediated gastrocnemius muscle hypertrophy and VEGF upregulation were not affected by 4 weeks of L-NAME treatment (online-only Supplemental Figure 1C and D). Similarly, treatment with L-NAME exhibited no effect on eNOS phosphorylation in the border zone and remote zone of myocardium (online-only Supplemental Figure 1E). Chronic L-NAME treatment also exacerbated acute mortality after MI because of increased incidence of cardiac rupture; however, there was no significant difference in the survival frequencies after MI between control and Akt1 TG mice (Figure 6C).

As revealed by echocardiography, the protective effect of skeletal muscle Akt1 activation on cardiac remodeling and systolic function was abolished by L-NAME treatment at both 2 and 4 weeks after transgene activation (Figure 6D). Hemodynamic measurements revealed that left ventricular systolic function, reflected by  $dP/dt_{max}$ , was not improved in Akt1 TG mice at 4 weeks after L-NAME treatment (Figure 6E). As shown in Figure 6F, the increase in heart weight/BW and lung wet weight/BW ratio at 4 weeks after MI was not different between control and Akt1 TG mice with chronic L-NAME treatment. These results indicate that the protective effect of Akt1-mediated muscle growth on cardiac dysfunction and remodeling is dependent on the activation of eNOS-derived nitric oxide.

## Discussion

It has been established that the Akt1 signaling pathway plays an important role in skeletal muscle hypertrophy in vitro and in vivo.<sup>28,29</sup> We previously generated a tetracycline-inducible skeletal muscle-specific Akt1 transgenic mouse model that displays a phenotype of increased fast/glycolytic type IIb but not slow/oxidative, muscle fiber growth.<sup>20</sup> Glycolytic type IIb fibers undergo hypertrophy in response to anabolic stimuli or resistance exercise, and they confer rapid and powerful contractions. Accordingly, these mice display superior grip strength but a slightly diminished capacity for endurance exercise.<sup>20</sup> Using this inducible transgenic system, the present study demonstrates that an Akt1-mediated, 5% increase of lean muscle mass can attenuate cardiac remodeling and dysfunction in a mouse MI model. Although Akt1 transgene expression was confined to skeletal muscle, there was an accompanying increase in myocardial capillary density and decrease in interstitial fibrosis. Akt1-mediated skeletal muscle growth also led to reductions in heart weight/BW and lung wet weight/BW ratios and decreased B-type natriuretic peptide expression. These data suggest that the level of lean muscle mass can determine the degree of cardiac remodeling in response to chronic ischemia.

In this study, we found that the improvement in LV remodeling resulting from muscle growth was accompanied by an increase in capillary density in the heart. It has been proposed that interventions aimed at increasing angiogenesis represent a promising strategy for treatment of heart disease.<sup>30</sup> We and others demonstrated that skeletal muscle growth affects systemic metabolism and cardiovascular disease partly through the production of muscle-derived secreted proteins, referred to as myokines.<sup>31,32</sup> For example, myogenic Akt1 signaling controls VEGF synthesis in skeletal muscle.<sup>26</sup> Consistent with this hypothesis, we found that levels of a number of angiogenic growth factors are increased in serum following transgene activation, including VEGF-A, SDF-1, FGF-1, and FGF2. This increase in angiogenic growth factor production was associated with an increase in the activating phosphorylation of eNOS at Ser1177 in heart. Because eNOS is proangiogenic,<sup>33</sup> these data are consistent with the increase in myocardial capillary density in response to Akt1 induction in skeletal muscle.

In contrast to the skeletal muscle hypertrophy model described here, the effect of endurance exercise training has been shown to attenuate MI-induced myocardial remodeling. Clinical studies have reported that aerobic endurance exercise training increases in exercise capacity and diminishes the unfavorable remodeling after acute myocardial infarction.<sup>34–36</sup> In rodent models, endurance exercise by voluntary treadmill running or graduated swim training have been shown to attenuate the MI-induced LV dysfunction.<sup>37,38</sup> The anti-remodeling effects were suggested to be the result of improved cardiac  $\beta$ 1-adrenergic signaling and myofilament function, and increased expression of the myocardial sarcoplasmic reticulum Ca pump and sarcolemmal Na-Ca exchanger proteins. Voluntary wheel running or swimming training before MI is also reported to reduce scar size increase capillary density and improve heart function during the remodeling phase in rodent models.<sup>39,40</sup>

Recently, de Waard and colleagues<sup>41</sup> demonstrated that the beneficial effects of endurance exercise after MI on LV remodeling and dysfunction depend critically on endogenous eNOS. Here it is shown that an increase in skeletal mass by Akt1 activation, independent of exercise training, is sufficient to confer cardioprotection in an experimental model of MI. Notably, the cardioprotective effect of Akt1-mediated skeletal muscle growth was lost by eNOS inhibition. Whereas the protective action of muscle growth was abolished by L-NAME treatment, the inhibition of eNOS did not promote post-MI remodeling in nontransgenic mice (compare Figures 2 and 6). Consistent with these findings, it has been reported that ablation of eNOS does not aggravate myocardial remodeling and LV dysfunction in MI models.<sup>41,42</sup>

While these data highlight an important role for eNOS in the protective actions of Akt1-mediated skeletal muscle growth on the heart, a number of questions remain. We detect an increase in eNOS activation in the heart in response to skeletal muscle growth, but we cannot rule out the possibility that it is systemic (versus cardiac) eNOS that confers the protective effect in this model; however, systemic eNOS may not be a main contributor for the therapeutic effects of Akt1-mediated muscle growth on cardiac remodeling, because an elevation of blood pressure by L-NAME treatment is similar in control and Akt1 TG mice. Furthermore, the mechanism by which eNOS becomes activated in response to the increase in skeletal muscle mass is unclear. It is possible that this effect is mediated by one or more of the angiogenic growth factors produced in response to muscle growth, but additional studies will be required to define these mechanisms.

Endurance training leads to an increase in mitochondrial content and oxidative capacity in muscle. On the other hand, anabolic stimuli lead to the hypertrophy of fast/glycolytic fibers, resulting in an increase in lean mass. Past the age of 30, approximately 3 kg of muscle mass, predominantly the fast/glycolytic fibers, are lost per decade of life.<sup>43</sup> We speculate that the loss of fast/glycolytic muscle may contribute to various age-related cardiovascular diseases. In this regard, it is widely recognized that muscle wasting is a strong independent risk factor for mortality in patients with heart failure,<sup>1</sup> and this is associated with a reduction in Akt signaling in muscle.<sup>19</sup> Several mouse models that show increased muscle mass have been generated by genetic alterations or pharmacological interventions<sup>44–46</sup>; however, the effect of increase in muscle mass (mediated predominantly by the hypertrophy glycolytic fibers) on cardiac diseases has not been investigated previously. In this study, we provide evidence in support of the hypothesis that a modest increase in fast/glycolytic skeletal muscle mass can attenuate cardiac remodeling after MI. Given that elderly patients are more likely than young patients to develop heart failure following MI,<sup>47</sup> maintaining fast/glycolytic muscle may be a reasonable strategy to limit cardiac remodeling in this disease.

In summary, Akt1-mediated, fast/glycolytic skeletal muscle growth led to the attenuation of LV dysfunction and detrimental remodeling in a murine myocardial infarction model. These



data support the concept that resistance training represents an alternative exercise intervention to the CHF patients,<sup>13</sup> particularly in those who cannot perform conventional aerobic training. Because CHF is frequently associated with cachexia, these findings also indicate that CHF may lead to a vicious cycle of cachexia and cardiac dysfunction. Further analysis of this experimental system may lead to the identification of factors involved in inter-tissue communication between skeletal and cardiac myocytes that affect the course of muscle atrophy and cardiac remodeling.

## Supplementary Material

Refer to Web version on PubMed Central for supplementary material.

## Acknowledgments

We thank Saeko Tokunaga and Megumi Nagahiro for the excellent technical assistance.

**Sources of Funding** This work was supported in part by a Grant-in-Aid for young scientists (start-up, 20890170) to Y.I. from the Ministry of Education, Science, and Culture, Japan, and a grant (AG34972) from the National Institutes of Health to K.W.

## References

1. Anker SD, Ponikowski P, Varney S, Chua TP, Clark AL, Webb-Peploe KM, Harrington D, Kox WJ, Poole-Wilson PA, Coats AJ. Wasting as independent risk factor for mortality in chronic heart failure. *Lancet*. 1997; 349:1050–1053. [PubMed: 9107242]
2. Strassburg S, Springer J, Anker SD. Muscle wasting in cardiac cachexia. *Int J Biochem Cell Biol*. 2005; 37:1938–1947. [PubMed: 15927519]
3. Yan Z, Okutsu M, Akhtar YN, Lira VA. Regulation of exercise-induced fiber type transformation, mitochondrial biogenesis, and angiogenesis in skeletal muscle. *J Appl Physiol*. 2010; 110:264–274. [PubMed: 21030673]
4. Zierath JR, Hawley JA. Skeletal muscle fiber type: influence on contractile and metabolic properties. *PLoS Biol*. 2004; 2:e348. [PubMed: 15486583]
5. Caforio AL, Rossi B, Risaliti R, Siciliano G, Marchetti A, Angelini C, Crea F, Mariani M, Muratorio A. Type 1 fiber abnormalities in skeletal muscle of patients with hypertrophic and dilated cardiomyopathy: evidence of subclinical myogenic myopathy. *J Am Coll Cardiol*. 1989; 14:1464–1473. [PubMed: 2809005]
6. Piepoli MF, Davos C, Francis DP, Coats AJ. Exercise training meta-analysis of trials in patients with chronic heart failure (ExTraMATCH). *BMJ*. 2004; 328:189. [PubMed: 14729656]
7. Jessup M, Abraham WT, Casey DE, Feldman AM, Francis GS, Ganiats TG, Konstam MA, Mancini DM, Rahko PS, Silver MA, Stevenson LW, Yancy CW. 2009 focused update: ACCF/AHA Guidelines for the Diagnosis and Management of Heart Failure in Adults: a report of the American College of Cardiology Foundation/American Heart Association Task Force on Practice Guidelines: developed in collaboration with the International Society for Heart and Lung Transplantation. *Circulation*. 2009; 119:1977–2016. [PubMed: 19324967]
8. Kemi OJ, Loennechen JP, Wisloff U, Ellingsen O. Intensity-controlled treadmill running in mice: cardiac and skeletal muscle hypertrophy. *J Appl Physiol*. 2002; 93:1301–1309. [PubMed: 12235029]
9. Nader GA, Esser KA. Intracellular signaling specificity in skeletal muscle in response to different modes of exercise. *J Appl Physiol*. 2001; 90:1936–1942. [PubMed: 11299288]
10. Williamson DL, Gallagher PM, Carroll CC, Raue U, Trappe SW. Reduction in hybrid single muscle fiber proportions with resistance training in humans. *J Appl Physiol*. 2001; 91:1955–1961. [PubMed: 11641330]
11. Lebrasseur NK, Walsh K, Arany Z. Metabolic benefits of resistance training and fast glycolytic skeletal muscle. *Am J Physiol Endocrinol Metab*. 2010; 300:E3–E10. [PubMed: 21045171]

12. Srikanthan P, Karlamangla AS. Relative muscle mass is inversely associated with insulin resistance and prediabetes. Findings from the third National Health and Nutrition Examination Survey. *J Clin Endocrinol Metab.* 2011; 96:2898–2903. [PubMed: 21778224]
13. Williams MA, Haskell WL, Ades PA, Amsterdam EA, Bittner V, Franklin BA, Gulanick M, Laing ST, Stewart KJ. Resistance exercise in individuals with and without cardiovascular disease: 2007 update: a scientific statement from the American Heart Association Council on Clinical Cardiology and Council on Nutrition, Physical Activity, and Metabolism. *Circulation.* 2007; 116:572–584. [PubMed: 17638929]
14. Anker SD, Steinborn W, Strassburg S. Cardiac cachexia. *Ann Med.* 2004; 36:518–529. [PubMed: 15513302]
15. Shiojima I, Walsh K. Regulation of cardiac growth and coronary angiogenesis by the Akt/PKB signaling pathway. *Genes Dev.* 2006; 20:3347–3365. [PubMed: 17182864]
16. Atherton PJ, Babraj J, Smith K, Singh J, Rennie MJ, Wackerhage H. Selective activation of AMPK-PGC-1 $\alpha$  or PKB-TSC2-mTOR signaling can explain specific adaptive responses to endurance or resistance training-like electrical muscle stimulation. *Faseb J.* 2005; 19:786–788. [PubMed: 15716393]
17. Bolster DR, Kubica N, Crozier SJ, Williamson DL, Farrell PA, Kimball SR, Jefferson LS. Immediate response of mammalian target of rapamycin (mTOR)-mediated signalling following acute resistance exercise in rat skeletal muscle. *J Physiol.* 2003; 553:213–220. [PubMed: 12937293]
18. Sandri M, Sandri C, Gilbert A, Skurk C, Calabria E, Picard A, Walsh K, Schiaffino S, Lecker SH, Goldberg AL. Foxo transcription factors induce the atrophy-related ubiquitin ligase atrogin-1 and cause skeletal muscle atrophy. *Cell.* 2004; 117:399–412. [PubMed: 15109499]
19. Toth MJ, Ward K, van der Velden J, Miller MS, Vanburen P, Lewinter MM, Ades PA. Chronic heart failure reduces Akt phosphorylation in human skeletal muscle: relationship to muscle size and function. *J Appl Physiol.* 2011; 110:892–900. [PubMed: 21193562]
20. Izumiya Y, Hopkins T, Morris C, Sato K, Zeng L, Viereck J, Hamilton JA, Ouchi N, LeBrasseur NK, Walsh K. Fast/glycolytic muscle fiber growth reduces fat mass and improves metabolic parameters in obese mice. *Cell Metab.* 2008; 7:159–172. [PubMed: 18249175]
21. Grill MA, Bales MA, Fought AN, Rosburg KC, Munger SJ, Antin PB. Tetracycline-inducible system for regulation of skeletal muscle-specific gene expression in transgenic mice. *Transgenic Res.* 2003; 12:33–43. [PubMed: 12650523]
22. Shiojima I, Sato K, Izumiya Y, Schiekofer S, Ito M, Liao R, Colucci WS, Walsh K. Disruption of coordinated cardiac hypertrophy and angiogenesis contributes to the transition to heart failure. *J Clin Invest.* 2005; 115:2108–2118. [PubMed: 16075055]
23. Tinsley FC, Taicher GZ, Heiman ML. Evaluation of a quantitative magnetic resonance method for mouse whole body composition analysis. *Obes Res.* 2004; 12:150–160. [PubMed: 14742854]
24. Shibata R, Izumiya Y, Sato K, Papanicolaou K, Kihara S, Colucci WS, Sam F, Ouchi N, Walsh K. Adiponectin protects against the development of systolic dysfunction following myocardial infarction. *J Mol Cell Cardiol.* 2007; 42:1065–1074. [PubMed: 17499764]
25. Izumiya Y, Shiojima I, Sato K, Sawyer DB, Colucci WS, Walsh K. Vascular endothelial growth factor blockade promotes the transition from compensatory cardiac hypertrophy to failure in response to pressure overload. *Hypertension.* 2006; 47:887–893. [PubMed: 16567591]
26. Takahashi A, Kureishi Y, Yang J, Luo Z, Guo K, Mukhopadhyay D, Ivashchenko Y, Branellec D, Walsh K. Myogenic Akt signaling regulates blood vessel recruitment during myofiber growth. *Mol Cell Biol.* 2002; 22:4803–4814. [PubMed: 12052887]
27. Fulton D, Gratton JP, McCabe TJ, Fontana J, Fujio Y, Walsh K, Franke TF, Papapetropoulos A, Sessa WC. Regulation of endothelium-derived nitric oxide production by the protein kinase Akt. *Nature.* 1999; 399:597–601. [PubMed: 10376602]
28. Bodine SC, Stitt TN, Gonzalez M, Kline WO, Stover GL, Bauerlein R, Zlotchenko E, Scrimgeour A, Lawrence JC, Glass DJ, Yancopoulos GD. Akt/mTOR pathway is a crucial regulator of skeletal muscle hypertrophy and can prevent muscle atrophy in vivo. *Nat Cell Biol.* 2001; 3:1014–1019. [PubMed: 11715023]

29. Lai KM, Gonzalez M, Poueymirou WT, Kline WO, Na E, Zlotchenko E, Stitt TN, Economides AN, Yancopoulos GD, Glass DJ. Conditional activation of akt in adult skeletal muscle induces rapid hypertrophy. *Mol Cell Biol.* 2004; 24:9295–9304. [PubMed: 15485899]
30. Vale PR, Isner JM, Rosenfield K. Therapeutic angiogenesis in critical limb and myocardial ischemia. *J Interv Cardiol.* 2001; 14:511–528. [PubMed: 12053643]
31. Pedersen BK, Akerstrom TC, Nielsen AR, Fischer CP. Role of myokines in exercise and metabolism. *J Appl Physiol.* 2007; 103:1093–1098. [PubMed: 17347387]
32. Walsh K. Adipokines, myokines and cardiovascular disease. *Circ J.* 2009; 73:13–18. [PubMed: 19043226]
33. Murohara T, Asahara T, Silver M, Bauters C, Masuda H, Kalka C, Kearney M, Chen D, Symes JF, Fishman MC, Huang PL, Isner JM. Nitric oxide synthase modulates angiogenesis in response to tissue ischemia. *J Clin Invest.* 1998; 101:2567–2578. [PubMed: 9616228]
34. Dubach P, Myers J, Dziekan G, Goebbels U, Reinhart W, Vogt P, Ratti R, Muller P, Miettunen R, Buser P. Effect of exercise training on myocardial remodeling in patients with reduced left ventricular function after myocardial infarction: application of magnetic resonance imaging. *Circulation.* 1997; 95:2060–2067. [PubMed: 9133516]
35. Giannuzzi P, Temporelli PL, Corra U, Gattone M, Giordano A, Tavazzi L. Attenuation of unfavorable remodeling by exercise training in postinfarction patients with left ventricular dysfunction: results of the Exercise in Left Ventricular Dysfunction (ELVD) trial. *Circulation.* 1997; 96:1790–1797. [PubMed: 9323063]
36. Otsuka Y, Takaki H, Okano Y, Satoh T, Aihara N, Matsumoto T, Yasumura Y, Morii I, Goto Y. Exercise training without ventricular remodeling in patients with moderate to severe left ventricular dysfunction early after acute myocardial infarction. *Int J Cardiol.* 2003; 87:237–244. [PubMed: 12559545]
37. de Waard MC, van der Velden J, Bito V, Ozdemir S, Biesmans L, Boontje NM, Dekkers DH, Schoonderwoerd K, Schuurbijs HC, de Crom R, Stienen GJ, Sipido KR, Lamers JM, Duncker DJ. Early exercise training normalizes myofilament function and attenuates left ventricular pump dysfunction in mice with a large myocardial infarction. *Circ Res.* 2007; 100:1079–1088. [PubMed: 17347478]
38. Wisloff U, Loennechen JP, Currie S, Smith GL, Ellingsen O. Aerobic exercise reduces cardiomyocyte hypertrophy and increases contractility, Ca<sup>2+</sup> sensitivity and SERCA-2 in rat after myocardial infarction. *Cardiovasc Res.* 2002; 54:162–174. [PubMed: 12062372]
39. de Waard MC, Duncker DJ. Prior exercise improves survival, infarct healing, and left ventricular function after myocardial infarction. *J Appl Physiol.* 2009; 107:928–936. [PubMed: 19574503]
40. Freimann S, Scheinowitz M, Yekutieli D, Feinberg MS, Eldar M, Kessler-Icekson G. Prior exercise training improves the outcome of acute myocardial infarction in the rat. Heart structure, function, and gene expression. *J Am Coll Cardiol.* 2005; 45:931–938. [PubMed: 15766831]
41. de Waard MC, van Haperen R, Soullie T, Tempel D, de Crom R, Duncker DJ. Beneficial effects of exercise training after myocardial infarction require full eNOS expression. *J Mol Cell Cardiol.* 2010; 48:1041–1049. [PubMed: 20153335]
42. Liu YH, Xu J, Yang XP, Yang F, Shesely E, Carretero OA. Effect of ACE inhibitors and angiotensin II type 1 receptor antagonists on endothelial NO synthase knockout mice with heart failure. *Hypertension.* 2002; 39:375–381. [PubMed: 11882576]
43. Tzankoff SP, Norris AH. Effect of muscle mass decrease on age-related BMR changes. *J Appl Physiol.* 1977; 43:1001–1006. [PubMed: 606683]
44. Guo T, Jou W, Chanturiya T, Portas J, Gavrilova O, McPherron AC. Myostatin inhibition in muscle, but not adipose tissue, decreases fat mass and improves insulin sensitivity. *PLoS One.* 2009; 4:e4937. [PubMed: 19295913]
45. McPherron AC, Lawler AM, Lee SJ. Regulation of skeletal muscle mass in mice by a new TGF-beta superfamily member. *Nature.* 1997; 387:83–90. [PubMed: 9139826]
46. Wenz T, Rossi SG, Rotundo RL, Spiegelman BM, Moraes CT. Increased muscle PGC-1alpha expression protects from sarcopenia and metabolic disease during aging. *Proc Natl Acad Sci U S A.* 2009; 106:20405–20410. [PubMed: 19918075]

47. Ezekowitz JA, Kaul P, Bakal JA, Armstrong PW, Welsh RC, McAlister FA. Declining in-hospital mortality and increasing heart failure incidence in elderly patients with first myocardial infarction. *J Am Coll Cardiol.* 2009; 53:13–20. [PubMed: 19118718]

### CLINICAL PERSPECTIVE

It is appreciated that aerobic endurance exercise can attenuate unfavorable myocardial remodeling postmyocardial infarction (MI). In contrast, little is known about the effect of increasing skeletal muscle mass, typically achieved by resistance training, on these processes. It is widely recognized that the muscle wasting is a strong independent risk factor for mortality in patients with heart failure, and this is associated with a reduction in Akt signaling within skeletal muscle. Using an inducible transgenic system, the present study demonstrates that an Akt1-mediated, 5% increase of lean muscle mass can attenuate cardiac remodeling and dysfunction in a mouse MI model. Although Akt1 transgene expression was confined to skeletal muscle, there was an accompanying increase in myocardial capillary density and a reduction in cardiac fibrosis. Akt1-mediated skeletal muscle growth increased angiogenic growth factor levels in serum, and this was associated with an increase in the activating phosphorylation of eNOS in the heart. Inhibition of eNOS abolished the protective effects of skeletal muscle growth on post-MI cardiac remodeling. Our data suggest that post-MI remodeling of the heart can be controlled by skeletal muscle to cardiac communication. Because heart failure is frequently associated with a loss of muscle mass, our findings also indicate that a vicious cycle of cachexia and cardiac dysfunction may contribute to this disease process and that maintaining skeletal muscle may be a reasonable strategy to limit cardiac remodeling.



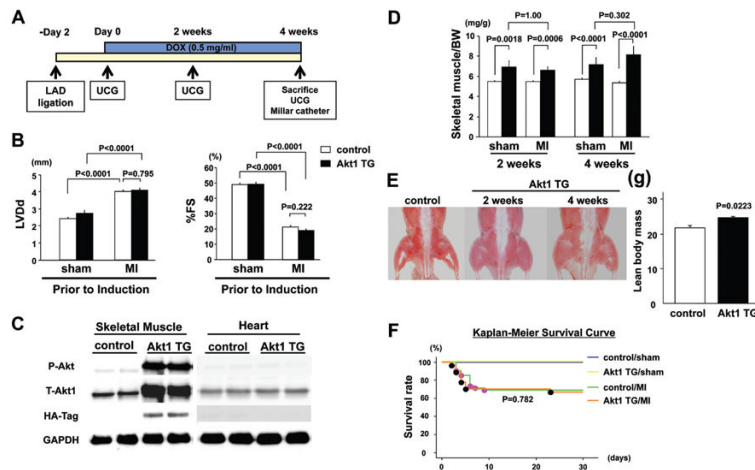


**Figure 1.**

**A**, Schematic illustration of experimental protocol and doxycycline (DOX)-treatment time course. **B**, Left ventricular (LV) diastolic dimension and percentage of fractional shortening in control and Akt1 transgenic (TG) mice 2 days after sham-operation or myocardial infarction (MI) ( $n=7$  mice per experimental group). **C**, Transgene expression following the addition of DOX. Representative blots of the gastrocnemius muscle and heart are shown. **D**, Gastrocnemius muscle weight in control and Akt1 TG mice at 2 and 4 weeks after DOX-treatment. **E**, Left: Representative gross appearance of control and Akt1 TG mice after 2 and 4 weeks of transgene induction. Right: Measurements of body composition after 2 weeks of transgene induction were made by quantitative magnetic resonance. **F**, Survival curves of control and Akt1 TG mice after MI and sham. Control/sham,  $n=15$ ; Control/MI,  $n=20$ ; Akt1 TG/sham,  $n=10$ ; Akt1 TG/MI,  $n=10$ . Results are presented as mean $\pm$ SEM. UCG indicates ultrasound cardiogram; LAD, left anterior descending artery.

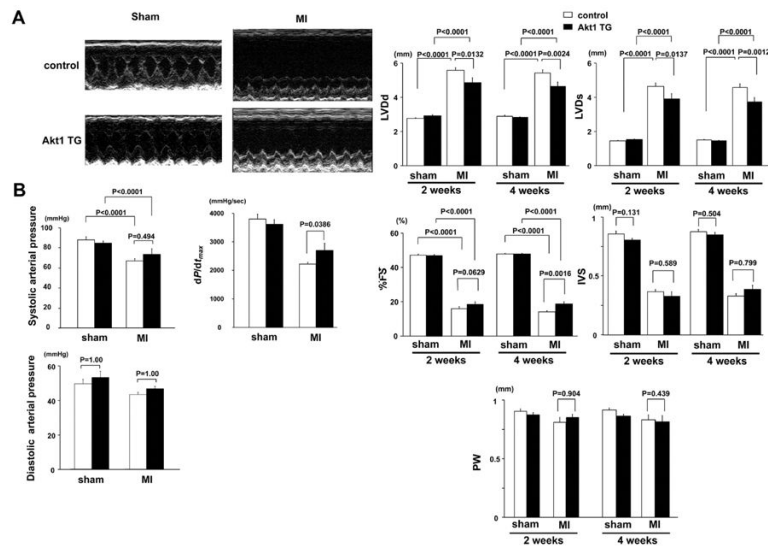


**Figure 2.** **A**, Top: Representative M-mode echocardiogram for control and Akt1 transgenic (TG) mice 4 weeks after sham-operation or myocardial infarction (MI). Bottom: Left ventricular (LV) diastolic dimension, LV systolic dimension, percentage of fractional shortening, intraventricular septum, and posterior wall in control and Akt1 TG mice 2 and 4 weeks after sham-operation or MI. **B**, Systolic and diastolic arterial blood pressure and  $dP/dt_{max}$  in control and Akt1 TG mice 4 weeks after sham-operation or MI. Results are presented as mean $\pm$ SEM (n=7 mice per experimental group).

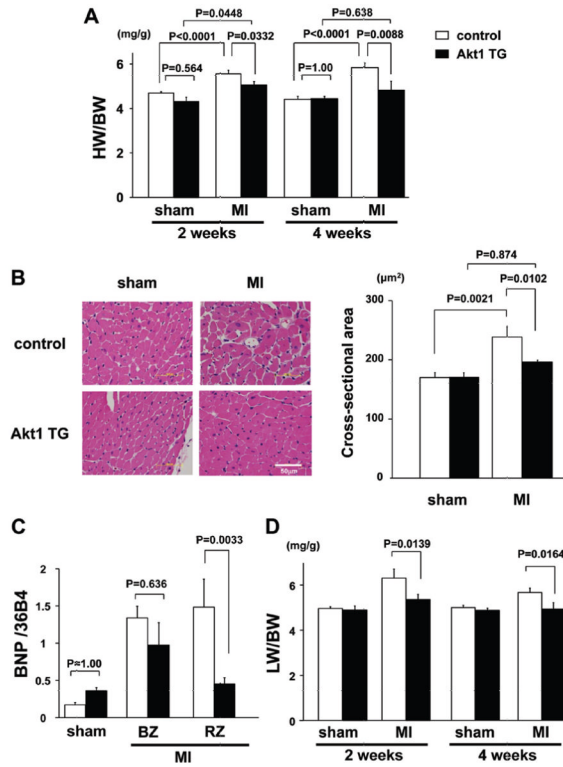


**Figure 3.**

**A**, Heart weight/body weight ratio in control and Akt1 transgenic (TG) mice at 2 and 4 weeks after doxycycline (DOX) treatment. **B**, Left: Representative images of hematoxylin and eosin-stained heart sections. Right: Quantitative analysis of cardiomyocyte cross-sectional area in control and Akt1 TG mice 2 weeks after sham-operation or myocardial infarction (MI). **C**, B-type natriuretic peptide mRNA expression in control and Akt1 TG mice at 2 weeks after DOX treatment. **D**, Lung wet weight/body weight ratio in control and Akt1 TG mice 2 and 4 weeks after sham-operation or MI. Results are presented as mean  $\pm$ SEM (n=7 mice per experimental group). BZ indicates border zone; RZ, remote zone.

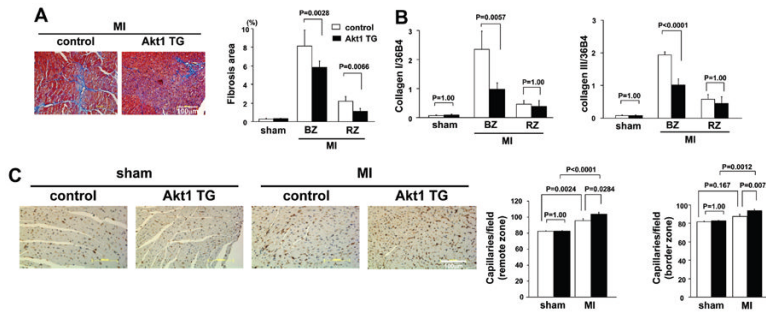


**Figure 4.** **A**, Left: Representative images of Masson's trichrome-stained heart sections. Right: Quantitative analysis of myocardial interstitial fibrosis in control and Akt1 transgenic (TG) mice at 2 weeks after transgene induction. **B**, Collagen I, III mRNA expression in control and Akt1 TG mice 2 weeks after sham operation or myocardial infarction (MI). **C**, Top: Representative images of anti-CD31-stained heart sections from remote zones. Bottom: Quantitative analysis of CD31-positive capillary density at border and remote zones in control and Akt1 TG mice at 2 weeks after doxycycline (DOX) treatment. Similar segments of the hearts were analyzed in sham-operated mice. Results are presented as mean±SEM (n=5 mice per experimental group).

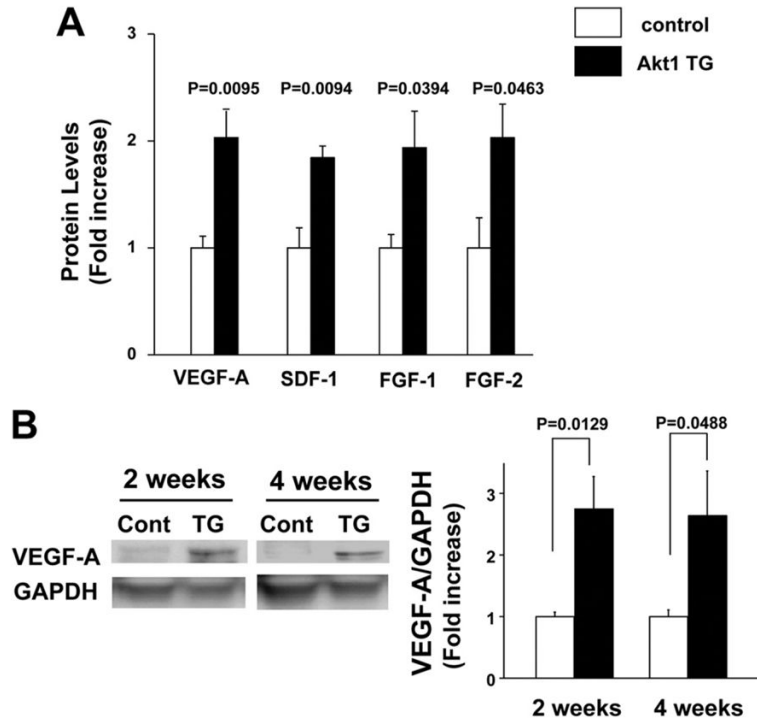


**Figure 5.** **A**, Quantitative analysis of serum angiogenesis-related protein levels in myocardial infarction (MI)-operated control and Akt1 transgenic (TG) mice 2 weeks after doxycycline (DOX) treatment by mouse angiogenesis protein arrays. Four independent experiments were quantified. **B**, Left: Representative immunoblots of vascular endothelial growth factor (VEGF) protein expression in gastrocnemius muscle 2 and 4 weeks after DOX treatment. Right: Quantitative analysis of immunoblots. Results are presented as mean±SEM (n=4).



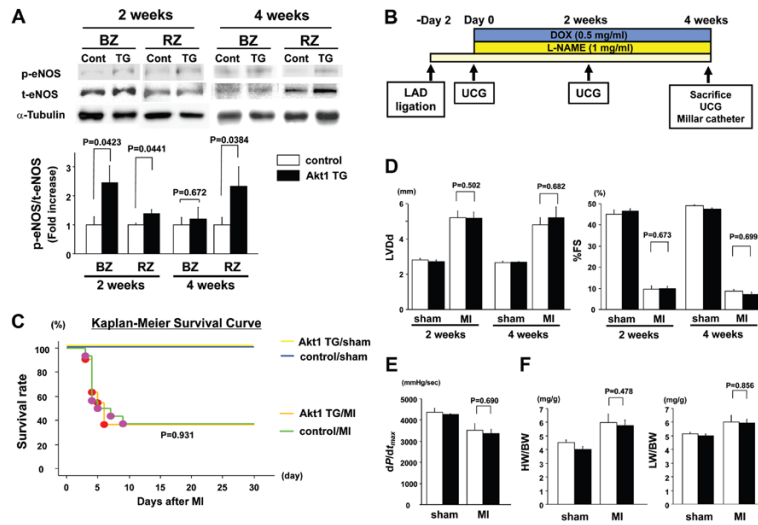


**Figure 6.**

**A**, Top: Representative immunoblots of p-eNOS, t-eNOS and  $\alpha$ -tubulin protein expression in the heart 2 and 4 weeks after doxycycline (DOX) treatment. Bottom: Quantitative analysis of immunoblots. **B**, Schematic illustration of experimental protocol of l-NAME and DOX-treatment time course. **C**, Survival curves of control and Akt1 transgenic (TG) mice after myocardial infarction (MI) and sham operation with l-NAME treatment. Control/sham, n=4; Akt1 TG/sham, n=4; Control/MI, n=16; Akt1 TG/MI, n=11. **D**, Left ventricular end-diastolic dimension and percentage of fractional shortening in control and Akt1 TG mice 2 and 4 weeks after MI with DOX and l-NAME treatment. **E**,  $dp/dt_{max}$  in control and Akt1 TG mice 4 weeks after MI with DOX and l-NAME treatment. **F**, Heart weight/body weight and lung wet weight/body weight ratio in control and Akt1 TG mice at 4 weeks after DOX and l-NAME treatment. Results are presented as mean $\pm$ SEM. BZ indicates border zone; RZ, remote zone; UCG, ultrasound cardiogram; LAD, left anterior descending artery; DOX, doxycycline.

**Table 1**

## Primer Sequences Used for Quantitative Real-Time PCR

Gene	Primer Sequences
BNP	
Forward	5'-GGAGTCCTAGCCAGTCTCC-3'
Reverse	5'-TTGGTCCTTCAAGAGCTGTC-3'
Collagen I	
Forward	5'-GTCCCAACCCCAAAGAC-3'
Reverse	5'-CATCTTCTGAGTTTGGTGATACGT-3'
Collagen III	
Forward	5'-GTCCCAACCCCAAAGAC-3'
Reverse	5'-CATCTTCTGAGTTTGGTGATACGT-3'
36B4	
Forward	5'-GCTCCAAGCAGATGCAGCA-3'
Reverse	5'-CCGGATGTGAGGCAGCAG-3'

**Table 2**

Body Weight, Heart Rate, and Mean Arterial Pressure in Experimental Groups of Mice

	Sham			MI		
	Control	Akt1 TG	<i>P</i> Value	Control	Akt1 TG	<i>P</i> Value
BW (g)	30.1±0.7	30.7±0.8	0.876	29.5±0.7	30.3±1.1	0.343
HR (bpm)	670±11	641±17	0.418	687±12	680±13	0.711
mAP (mm Hg)	63.0±2.7	65.9±3.7	0.631	54.2±1.1	58.2±1.1	0.189

Results are presented as mean±SEM. Measurements were made at 4 weeks post-surgery.